JVI Journals.ASM.org

Proteomic Analysis of Ubiquitin-Like Posttranslational Modifications Induced by the Adenovirus E4-ORF3 Protein

Sook-Young Sohn, Rebecca G. Bridges, Patrick Hearing

Department of Molecular Genetics and Microbiology, School of Medicine, Stony Brook University, Stony Brook, New York, USA

ABSTRACT

Viruses interact with and regulate many host metabolic pathways in order to advance the viral life cycle and counteract intrinsic and extrinsic antiviral responses. The human adenovirus (Ad) early protein E4-ORF3 forms a unique scaffold throughout the nuclei of infected cells and inhibits multiple antiviral defenses, including a DNA damage response (DDR) and an interferon response. We previously reported that the Ad5 E4-ORF3 protein induces sumoylation of Mre11 and Nbs1, which are essential for the DDR, and their relocalization into E4-ORF3-induced nuclear inclusions is required for this modification to occur. In this study, we sought to analyze a global change in ubiquitin-like (Ubl) modifications, with particular focus on SUMO3, by the Ad5 E4-ORF3 protein and to identify new substrates with these modifications. By a comparative proteome-wide approach utilizing immunoprecipitation/mass spectrometry, we found that Ubl modifications of 166 statistically significant lysine sites in 51 proteins are affected by E4-ORF3, and the proteome of modifications spans a diverse range of cellular functions. Ubl modifications of 92% of these identified sites were increased by E4-ORF3. We further analyzed SUMO3 conjugation of several identified proteins. Our findings demonstrated a role for the Ad5 E4-ORF3 protein as a regulator of Ubl modifications and revealed new SUMO3 substrates induced by E4-ORF3.

IMPORTANCE

The adenovirus E4-ORF3 protein induces dynamic structural changes in the nuclei of infected cells and counteracts host antiviral responses. One of the mechanisms that accounts for this process is the relocalization and sequestration of cellular proteins into an E4-ORF3 nuclear scaffold, but little is known about how this small viral protein affects diverse cellular responses. In this study, we analyzed for the first time the global pattern of ubiquitin-like (Ubl) modifications, with particular focus on SUMO3, altered by E4-ORF3 expression. The results suggest a role for the Ad5 E4-ORF3 protein as a regulator of Ubl modifications and reveal new SUMO3 substrates targeted by E4-ORF3. Our findings propose Ubl modifications as a new mechanism by which E4-ORF3 may modulate cellular protein functions in addition to subnuclear relocalization.

Viruses interact with and regulate many host metabolic pathways to advance the viral life cycle and counteract intrinsic and extrinsic antiviral responses. Numerous examples with different DNA and RNA virus families demonstrate how viruses regulate host transcription, translation, DNA replication, and in certain cases, host cell posttranslational modifications. During adenovirus (Ad) infection, host cell DNA replication and translation are shut off in order to promote replication of the viral genome and translation of viral proteins. Additionally, Ad counteracts several intrinsic and interferon (IFN)-induced cellular, antiviral responses. For example, Ad infection triggers a cellular DNA damage response (DDR) that may impede the virus life cycle (1). The Ad virus particle contains a linear, double-stranded DNA genome of ~36 kbp in length. The open ends of this linear DNA are perceived by the infected cell as DNA damage, and a DDR may occur following Ad infection. If unabated, the cellular DDR actively inhibits viral DNA replication, in part by ligation of the viral DNA in an end-to-end manner which masks and mutates the origins of viral DNA replication. This process may block the entire viral replication cycle (1, 2). Therefore, Ad has evolved several mechanisms to inhibit the cellular DDR early after infection. The incoming viral genome is coated with a basic viral core protein that may block recognition of the viral DNA by the cellular DDR machinery at the earliest stages of infection (3). Once Ad early protein synthesis ensues, two distinct mechanisms are employed to inhibit the DDR (1, 2). The Ad5 E1B-55K and E4-ORF6 proteins form an E3 ubiquitin (Ub) ligase complex with cellular proteins cullin 5 (CUL5), Rbx1, and elongins B and C (4, 5). Together, this complex leads to ubiquitin-mediated, proteasome-dependent degradation of cellular sensors of DNA damage, including Mre11, Rad50, and Nbs1 (the MRN complex) (6). Inhibition of cellular sensors of DNA damage blocks downstream signaling events and inhibits both DNA damage repair and cell cycle checkpoint signaling. The Ad5 E4-ORF3 protein sequesters MRN proteins into nuclear inclusions, termed nuclear tracks (7), within infected cell nuclei to inhibit MRN activity (6, 8). E4-ORF3 recruits numerous nuclear proteins into these structures, including promyelocytic leukemia (PML) and other PML-nuclear body (PML-NB)-associ-

Received 3 October 2014 **Accepted** 13 November 2014

Accepted manuscript posted online 19 November 2014

Citation Sohn S-Y, Bridges RG, Hearing P. 2015. Proteomic analysis of ubiquitin-like posttranslational modifications induced by the adenovirus E4-ORF3 protein. J Virol 89:1744–1755. doi:10.1128/JVI.02892-14.

Editor: M. J. Imperiale

Address correspondence to Patrick Hearing, patrick.hearing@stonybrook.edu.

Supplemental material for this article may be found at http://dx.doi.org/10.1128/JVI.02892-14.

doi:10.1128/JVI.02892-14

ated proteins, such as Sp100 and Daxx, to inactivate cellular antiviral defense mechanisms induced by interferon (9, 10).

We previously reported that Ad5 induces SUMO (small ubiquitin-like modifier) modification of Mre11 and Nbs1 during the early phase of infection (11). We found that the E4-ORF3 protein is both necessary and sufficient to induce Mre11 and Nbs1 SUMO conjugation. Relocalization of Mre11 and Nbs1 into E4-ORF3-induced nuclear inclusions is required for this modification to occur. Upon wild-type Ad5 infection, Mre11 and Nbs1 sumoylation reaches a peak at early times after infection and declines thereafter. SUMO1 deconjugation from Nbs1 depends on degradation of Mre11 by the viral E1B-55K–E4-ORF6 E3 ubiquitin ligase complex, whereas SUMO2 deconjugation is independent of viral early gene products. Inhibition of viral DNA replication blocks SUMO2 deconjugation from Mre11 and Nbs1, indicating that a late-phase process is involved in their desumoylation. Our results provide direct evidence of Mre11 and Nbs1 sumoylation induced by the Ad5 E4-ORF3 protein and an important example that modification of a single substrate by both SUMO1 and SUMO2 is regulated through distinct mechanisms (11). These findings suggest E4-ORF3-mediated relocalization of the MRN complex influences the cellular DNA damage response.

Posttranslational modification by SUMO is associated with the regulation of diverse cellular processes, including transcription, proliferation, apoptosis, the DDR, subcellular localization, protein stability, and intrinsic and innate immunity to pathogens (12, 13). Vertebrates encode four SUMO isoforms: SUMO1 through SUMO4. SUMO1, SUMO2, and SUMO3 are ubiquitously expressed, whereas SUMO4 expression is found primarily in cells of the immune system (12, 13). SUMO2 and SUMO3 have 95% amino acid homology in precursor form and 97% homology in mature form and are frequently referred to as SUMO2/3. SUMO1 and SUMO2/3 have only 50% homology and typically have unique substrate specificity. It is thought that in contrast to SUMO1, SUMO2/3 modification is regulated more dynamically in response to various stimuli, such as heat shock, oxidative stress, and pathogens, since the unconjugated, free SUMO2/3 population is larger than the free SUMO1 population in mammalian cells (12, 13). SUMO proteins are synthesized as precursors that are cleaved after a C-terminal diglycine (GG) sequence by cellular SUMO proteases (SENPs). SUMO proteins are members of the ubiquitin-like (Ubl) family that also includes Nedd8, ISG15, and FAT10. These Ubls are small proteins, ~100 amino acids long, and are conjugated via a C-terminal glycine residue to the epsilon amine group of a lysine residue in the target substrate (K-ε-GG linkage). Covalent attachment of SUMO to a substrate occurs via a pathway analogous to the ubiquitin conjugation system. Processed SUMO is covalently linked to an E1-activating enzyme (SAE-1:SAE-2) via a thioester linkage between the E1 active site cysteine residue and the C-terminal SUMO glycine residue. SUMO is then transferred to an E2-conjugating enzyme (Ubc9 in humans). Ubc9 may directly transfer SUMO to a substrate or, alternatively, transfer SUMO to an E3 ligase followed by SUMO conjugation to a substrate. More than 10 SUMO E3 ligases have been described (12, 13). It remains unclear how the sumoylation system confers substrate specificity and SUMO paralog specificity to a wide range of substrates using only one E2 SUMO enzyme and a limited number of E3 SUMO ligases. Some SUMO conjugation sites share the consensus sequence Ψ-K-X-D/E (Ψ is a large hydrophobic amino acid and X is any amino acid), but an increasing number of substrate conjugation sites have been identified that do not contain this consensus sequence. SUMO1 is conjugated as a monomer, whereas SUMO2/3 may be conjugated as monomers or multimers (12, 13).

In this study, we sought to identify new substrates with ubiquitin-like modifications induced during the early phase of Ad infection by the E4-ORF3 protein. To date, only Mre11 and Nbs1 have been identified as E4-ORF3-induced SUMO substrates (11). The E4-ORF3 protein predominantly induces SUMO2/3 conjugation of Mre11 and Nbs1 (11). The detection of sumoylation is significantly complicated by the activity of SENPs in cellular extracts. Most of the previously described approaches to identify sumoylated substrates and map SUMO conjugation sites involve cell lysis under denaturing conditions followed by one of a number of SUMO enrichment approaches (14–20). A method to map sumoylation sites by mass spectrometry (MS) was described that used a modified SUMO1 with an arginine residue engineered immediately N-terminal to the diglycine linkage site (21). Trypsin cleavage of sumoylated substrates linked to this SUMO1 variant resulted in the release of a signature peptide containing a diglycine remnant attached to the amine group of the target lysine residue (K-ε-GG) (21). An antibody was recently described that recognizes the same remnant motif of ubiquitin site conjugation following trypsin digestion, K-ε-GG (22). We engineered a cell line that constitutively expresses His_6-tagged SUMO3 in which the threonine at position 90 was changed to an arginine residue, SUMO3(T90R). SUMO3(T90R) was expressed at physiological levels, and the variant was found to be efficiently conjugated to both Mre11 and Nbs1 following wild-type Ad5 infection. We utilized this cell line in an immunoprecipitation/mass spectrometry analysis to identify new substrates whose Ubl modification is altered by Ad5 E4-ORF3. E4-ORF3-induced sumoylation was verified with candidate substrates, and new sumoylation substrates were identified by these analyses.

MATERIALS AND METHODS

Plasmid and cell line. To generate a His_6-SUMO3(T90R) expression vector, Thr^{90} of human SUMO3 in a pcDNA3 vector, was replaced with an Arg residue by site-directed mutagenesis. HeLa cells were cotransfected with pcDNA-His_6-SUMO3(T90R) and pSilencer 2.1-U6 puro by using polyethylenimine (PEI; Polysciences) and selected with neomycin (50 μg/ml) and puromycin (1 μg/ml). The presence of His_6-SUMO3(T90R) in the selected cell line was confirmed by PCR and sequencing.

Antibodies. The rat monoclonal antibody 6A11 against adenovirus E4-ORF3 (23) was provided by T. Dobner (Heinrich-Pette Institute). The anti-DBP (B6-8) mouse monoclonal antibody was from A. J. Levine (Princeton University), and the rabbit polyclonal anti-DBP antibody was from P. van der Vliet (University of Utrecht). The anti-TIF1γ rabbit polyclonal antibody was described previously (24). The anti-His_6 (H-15) and anti-PML (H-238) rabbit polyclonal antibodies and anti-E1A (M73) and anti-RanGAP1 (C-5) mouse monoclonal antibodies were purchased from Santa Cruz Biotechnology. The anti-Nbs1 mouse monoclonal antibody was from GeneTex, the anti-Mre11 rabbit polyclonal antibody was from Novus, the anti-SUMO1 and anti-SUMO2/3 rabbit polyclonal antibodies were from Zymed, the anti-Ubiquitin mouse monoclonal antibody was from Stressgen, the anti-ISG15 and anti-TFII-I rabbit polyclonal antibodies were from Cell Signaling Technology, and the anti-Nedd8 rabbit polyclonal antibody was from BioMol.

Immunoprecipitation. His_6-SUMO3-expressing HeLa cells (10^7) were uninfected or infected with either wild-type or E4-ORF3-deficient Ad5. At 7 h postinfection, cells were washed with phosphate-buffered saline (PBS), lysed in 0.3 ml of SDS lysis buffer (1% SDS, 10 mM Tris [pH

8.0], 150 mM NaCl, 1 mM EDTA, and 1 mM phenylmethylsulfonyl fluoride [PMSF]), and boiled for 10 min. After centrifugation at 12,000 × *g* for 10 min, 1.2 ml of immunoprecipitation (IP) dilution buffer (10 mM Tris [pH 8.0], 150 mM NaCl, 1 mM EDTA, 1% Triton X-100, and 1 mM PMSF) was added to the supernatant. Lysates were precleared with protein G-agarose beads (Roche Applied Science) for 1 h and incubated overnight with either mouse IgG or mouse anti-Ub antibody (Stressgen), followed by incubation with protein G-agarose for 3 h. The beads were washed five times with IP dilution buffer and analyzed by 7.5% SDS-PAGE and Western blotting.

***In vivo* sumoylation assay.** The parent HeLa cells or His_6-tagged SUMO3-expressing HeLa cells were uninfected or infected with wild-type or E4-ORF3-deficient Ad5 for 7 h, and SUMO conjugates were prepared and analyzed as described previously (20).

Immunofluorescence. For immunofluorescence analysis, the cells were grown on glass coverslips in a 24-well plate and fixed in methanol. After blocking in PBS containing 10% goat serum, cells were stained with the indicated antibodies. The Alexa 488-conjugated anti-mouse secondary antibody was from Molecular Probes, and the fluorescein isothiocyanate-conjugated anti-rabbit and tetramethyl rhodamine isothiocyanate-conjugated anti-rat, anti-mouse, and anti-rabbit secondary antibodies were from Zymed. Nuclei were visualized by 4′,6-diamidino-2-phenylindole (DAPI) staining. Cell images were acquired on an Axiovert 200M digital deconvolution microscope (Zeiss) and analyzed using Axiovision software.

Cell preparation, protein extraction, and digestion. His_6-SUMO3 (T90R)-expressing HeLa cells (2×10^8) were infected with 200 particles per cell of wild-type Ad5 or E4-ORF3-deficient Ad5 for 1 h. At 7 h postinfection, cells were washed three times with PBS and collected by centrifugation at 2,000 × *g*. Cell pellets were flash-frozen in liquid nitrogen and shipped on dry ice to Cell Signaling Technology Inc. (Danvers, MA) for UbiScan analysis by using the Ubiquitin Remnant Motif K-ε-GG rabbit monoclonal antibody (antibody 5562). Cells were lysed in urea lysis buffer (20 mM HEPES [pH 8.0], 9.0 M urea, 1 mM sodium orthovanadate, 2.5 mM sodium pyrophosphate, and 1 mM glycerol-phosphate). Sonication of cell lysates was applied at 15 W output power twice for 20 s and once for 15 s. The resulting lysates were centrifuged at 20,000 × *g* for 15 min to remove insoluble material. Protein extracts were reduced and carboxamidomethylated. After normalizing total protein for each sample, proteins were digested overnight using trypsin. Resulting peptides were separated from nonpeptide material by solid-phase extraction with Sep-Pak C_{18} cartridges. Lyophilized peptides were resuspended in morpholinepropanesulfonic acid (MOPS) immunoaffinity purification buffer (50 mM MOPS [pH 7.2], 10 mM KH_2PO_4, and 50 mM NaCl) and clarified by centrifugation. Supernatants were mixed with slurries of immobilized PTMScan ubiquitin branch K-ε-GG motif antibody for 2.5 h at 4°C. Beads were pelleted by centrifugation and washed once in MOPS immunoaffinity purification buffer and four times with water. Peptides were eluted from beads with two sequential incubations in 0.15% trifluoroacetic acid (TFA), 10 min each, at room temperature. Eluted peptides were desalted over tips filled with C_{18} packing material, eluted with 60% acetonitrile in 0.1% TFA, and lyophilized.

Liquid chromatography-tandem mass spectrometry (LC-MS/MS) analysis. The samples were run in duplicate to generate analytical replicates and increase the number of MS/MS identifications from each sample. Immunoprecipitated peptides were resuspended in 0.125% formic acid and loaded directly onto a 10-cm by 75-m PicoFrit capillary column packed with Magic C_{18} AQ reverse-phase resin. The column was developed with a 90-min linear gradient of acetonitrile in 0.125% formic acid delivered at 280 nl/minute. Tandem mass spectra were collected with an linear trap quadropole (LTQ)-Orbitrap Velos hybrid mass spectrometer running XCalibur software (version 2.0.7; SP1) using a top 20 MS/MS method, a dynamic exclusion repeat count of one, and a repeat duration of 30 s. Real-time calibration of mass error was performed using lock mass with a singly charged polysiloxane ion with *m/z* 371.101237 (25). MS spectra were collected in the Orbitrap component of the mass spectrometer, and MS/MS spectra were collected with the LTQ component.

Data analysis. Data processing was performed as described previously (25). MS/MS spectra were evaluated using SEQUEST 3G and the SORCERER 2 platform from Sage-N Research (version 4.0; Milpitas, CA) (26). Searches were performed against the most recent update of the NCBI *Homo sapiens* FASTA database (updated on 6 September 2010; release 43) containing 39,112 sequences, and the human adenovirus type 5 genome (AC_000008; updated on 8 December 2008), containing 36 sequences. A mass accuracy of ±50 ppm was used for precursor ions and ±1.0 Da for product ions. Enzyme specificity was limited to trypsin, with at least one tryptic (lysine or arginine)-containing terminus required per peptide and up to four missed cleavages allowed. Cysteine carboxamidomethylation was specified as a static modification, and oxidation of methionine was allowed as a variable modification. Results were filtered with a mass accuracy of ±5 ppm on precursor ions and presence of the intended K-ε-GG motif. Reverse decoy databases were included for all searches to estimate false-positive rates, and peptide assignments were obtained using a 5% false-positive discovery rate in the Peptide Prophecy module of SORCERER 2 (27). The results were further narrowed by applying a mass accuracy filter of ±5 ppm of calculated *m/z* values, depending on the distribution and symmetry of the XCorr-versus-ppm plot for a given search result.

RESULTS

Validation of the SUMO3(T90R) cell line. We sought to identify sites of SUMO conjugation altered by the E4-ORF3 protein during Ad5 infection by using a recently described antibody that recognizes the remnant motif of ubiquitin conjugation following trypsin digestion: K-ε-GG (PTMScan ubiquitin remnant motif antibody; Cell Signaling Technology [28]). A lysine or arginine residue was not present at the N terminus of the GG residues in any of the SUMO isoforms (Fig. 1A). Therefore, we engineered a cell line that constitutively expresses a His_6-tagged SUMO3 in which the threonine at position 90 was changed to an arginine residue (21), termed SUMO3(T90R); the GG residues in SUMO3 are present at positions 91 and 92 (Fig. 1A). SUMO3(T90R) was tagged at the N terminus with His_6 to allow for protein purification under denaturing conditions using Ni-nitrilotriacetic acid (NTA)–agarose beads (20). A HeLa cell clone expressing His_6-SUMO3(T90R) at physiological levels relative to total SUMO2/3 levels in HeLa cells (Fig. 1B) was selected and used for subsequent experiments. The His_6-SUMO3(T90R) expression level was similar to that found in a previously described HeLa cell line expressing His_6-SUMO3 (20) (Fig. 1B). His_6-SUMO3- or His_6-SUMO3(T90R)-expressing HeLa cells were left uninfected or infected with wild-type Ad5 or E4-ORF3-deficient Ad5 (ΔE4-ORF3) for 7 h, and SUMO3 subcellular localization was evaluated by immunofluorescence. His_6-SUMO3 and His_6-SUMO3(T90R) were diffusely localized in the nuclei of uninfected cells with some puncta evident (Fig. 1D). His_6-SUMO3 and His_6-SUMO3(T90R) were both relocalized into nuclear tracks containing the E4-ORF3 protein following infection with wild-type Ad5 (Fig. 1D). Neither His_6-SUMO3 nor His_6-SUMO3(T90R) protein was relocalized following infection with E4-ORF3-deficient Ad5 (Fig. 1D). We compared total SUMO3 conjugation patterns and Nbs1-specific SUMO3 conjugation patterns by using an *in vivo* sumoylation assay with His_6-SUMO3 and His_6-SUMO3(T90R) cells infected with wild-type Ad5 for 7 h. Total SUMO3 conjugation patterns were the same with His_6-SUMO3 and His_6-SUMO3(T90R) cells (Fig. 1C, lysate, bottom panel), as was the pattern of Ad5 E4-ORF3-induced sumoylation of Nbs1 (Fig. 1C, His pulldown, top

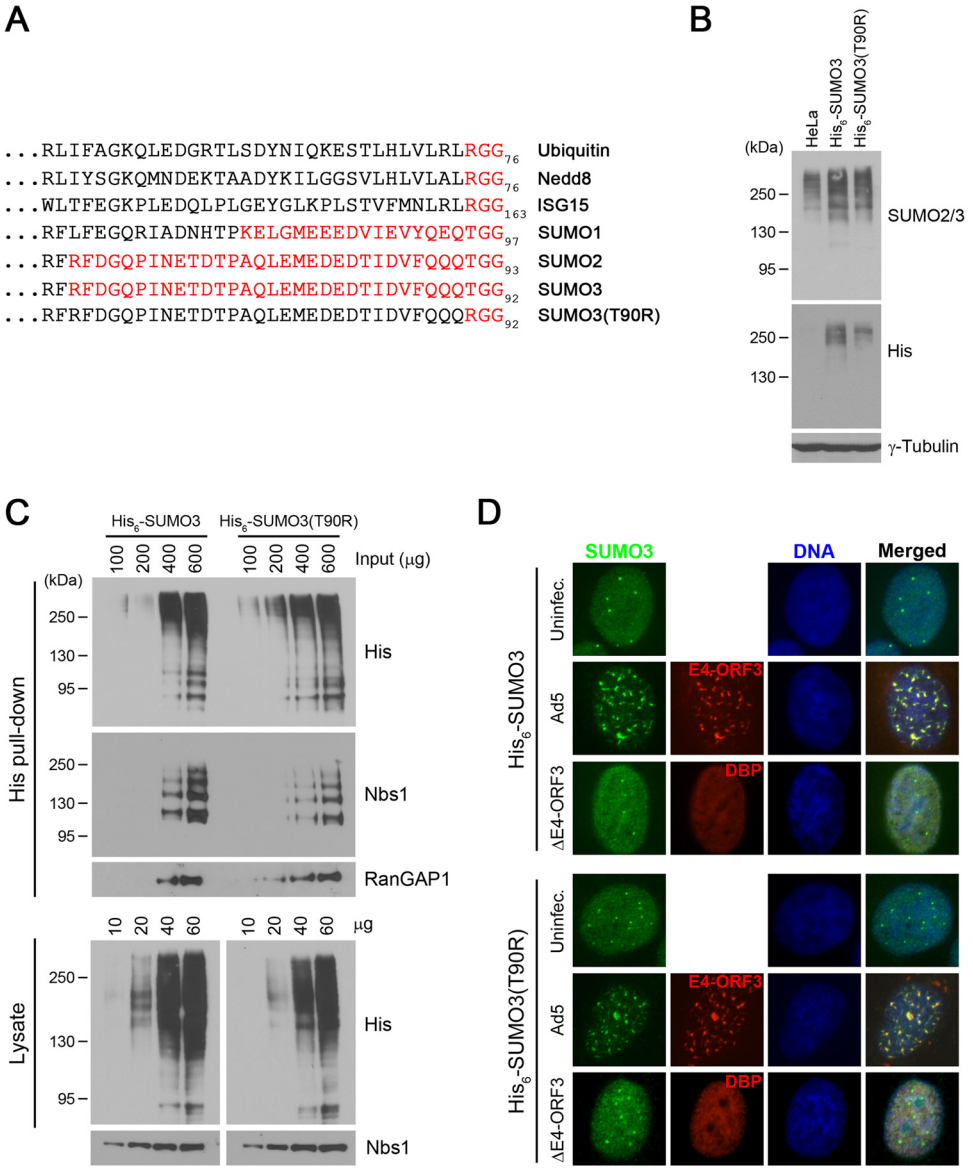

FIG 1 Validation of HeLa cell stable expression of His_6-SUMO3(T90R). (A) The amino acid sequences to the N terminus of the diglycine residues in mature ubiquitin, Nedd8, ISG15, SUMO1, SUMO2, SUMO3, and SUMO3(T90R) are shown. Peptides that would be generated following trypsin cleavage of a conjugated substrate are shown in red. (B) Expression levels of SUMO2/3 and His_6-tagged SUMO3 in parent HeLa and His_6-SUMO3 and His_6-SUMO3(T90R)-HeLa cells. Total cell lysates were analyzed by Western blotting with anti-SUMO-2/3, anti-His, and anti-γ-tubulin antibodies. Molecular mass markers are indicated on the left. (C) SUMO3 and SUMO3(T90R) conjugation to Nbs1 during Ad5 infection. Cells were infected with Ad5 for 7 h, SUMO conjugates were prepared using Ni-NTA–agarose beads under denaturing conditions, and increasing amounts of eluates were analyzed by Western blotting (His pulldown). RanGAP1 was analyzed as a sumoylation control. Increasing amounts of total cell lysates were analyzed by Western blotting with anti-Nbs1 and anti-His antibodies. (D) Subnuclear localization of His_6-SUMO3 (top three rows) and His_6-SUMO3(T90R) (bottom three rows) proteins. His_6-tagged SUMO3 and SUMO3(T90R)-expressing HeLa cells were uninfected or infected with wild-type or E4-ORF3-deficient Ad5 for 7 h. SUMO3 proteins were immunostained using the anti-His antibody. E4-ORF3 and E2-DBP were used as markers for infected cells. Nuclei were visualized by DAPI staining (DNA).

panel). RanGAP1, a major cellular SUMO substrate, served as a positive control for His_6-SUMO3 capture in this experiment. These results substantiate that His_6-SUMO3(T90R) is expressed at physiological levels in our HeLa cell line, and the T90R mutation of SUMO3 affects neither its conjugation properties nor subcellular localization in the absence or presence of Ad5 infection.

Proteomic identification of cellular proteins whose Ubl conjugation is regulated by Ad5 E4-ORF3. We aimed to identify new cellular substrates whose sumoylation is regulated by the Ad5 E4-ORF3 protein. To focus our screen on the specific effects of E4-ORF3 and to avoid potential effects of other Ad5 regulatory proteins on host posttranslational modifications, we compared wild-type Ad5-infected cells to cells infected with ΔE4-ORF3. We chose to compare Ubl conjugation patterns between these two viruses, since they are identical in viral protein expression, with the exception of the E4-ORF3 protein. We did not compare Ad5-infected cells to uninfected cells, since we anticipated that patterns of sumoylation, as well as ubiquitin and other Ubl modifications, un-

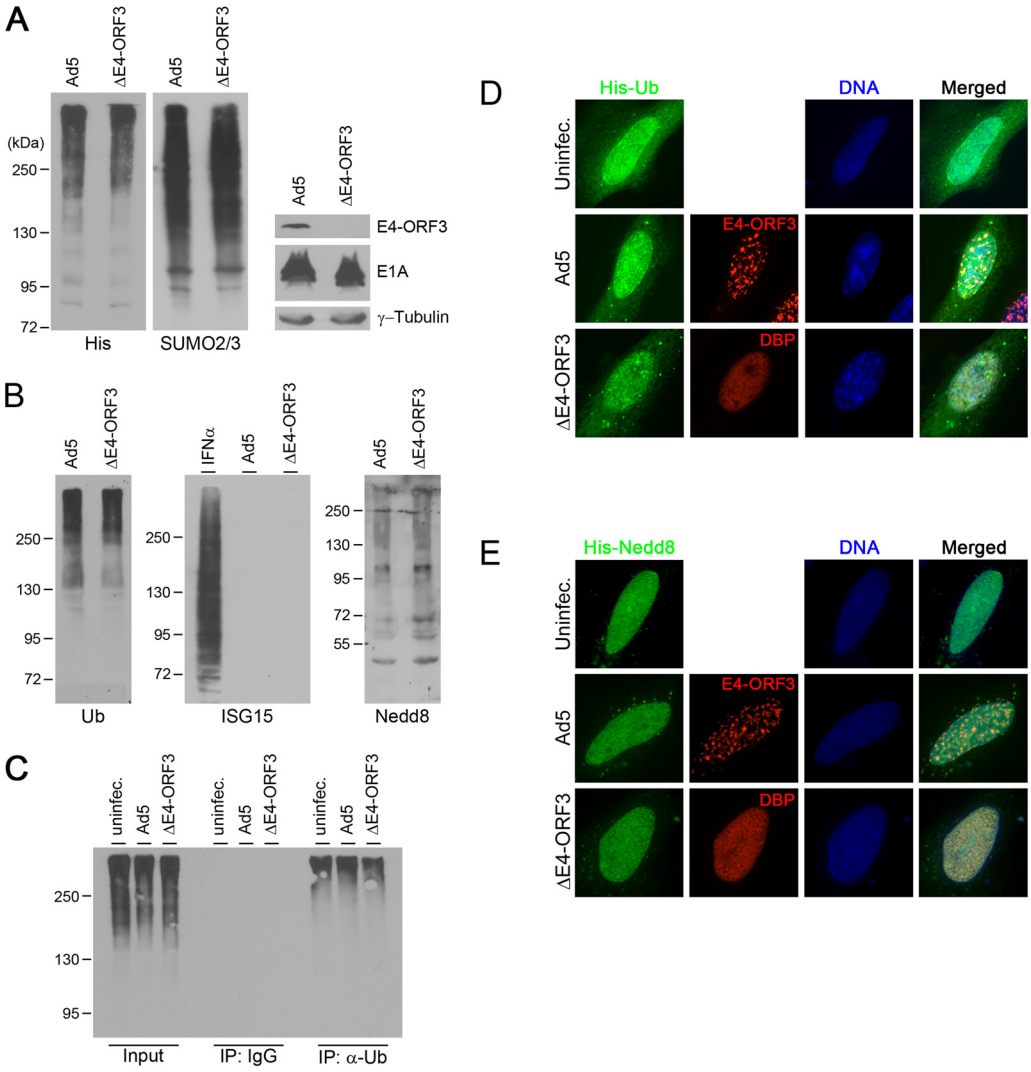

FIG 2 Analysis of ubiquitin and ubiquitin-like protein conjugation and localization during Ad5 infection. (A) Total SUMO2/3 and SUMO3(T90R) expression in HeLa-His_6-SUMO3(T90R) cells during wild-type and E4-ORF3-deficient Ad5 infection. Total cell lysates were prepared at 7 h postinfection and analyzed by Western blotting using anti-His, -SUMO2/3, -E4-ORF3, -E1A, and -γ-tubulin antibodies. (B) HeLa cells were infected with wild-type or E4-ORF3-deficient Ad5 for 7 h. Total cell lysates were prepared and analyzed by Western blotting with anti-ubiquitin, -ISG15, and -Nedd8 antibodies. For a positive control of ISG15 expression, cells were treated with interferon (500 U/ml) for 48 h. (C) Ubiquitination levels in His_6-SUMO3(T90R)-expressing HeLa cells during Ad infection. Total cell lysates from uninfected cells or cells infected with wild-type or E4-ORF3-deficient Ad5 were prepared (Input), and mouse IgG and anti-ubiquitin antibodies were used for immunoprecipitation (IP) followed by Western blotting using anti-ubiquitin antibody. (D) Subcellular localization of ubiquitin in Ad-infected HeLa cells. HeLa cells were transfected with a His_6-ubiquitin expression plasmid and left uninfected or infected with wild-type or E4-ORF3-deficient Ad5 for 7 h. Ubiquitin was immunostained with an anti-His_6 antibody, and E4-ORF3 and E2-DBP were used as markers for infected cells. Nuclei were visualized by DAPI staining (DNA). (E) Subcellular localization of His_{12}-Nedd8 in Ad-infected HeLa cells. The analysis was performed as described for that shown in panel D.

related to E4-ORF3 expression might change, since the process of viral infection itself induces cellular signaling, including the mitogen-activated protein (MAP) kinase and integrin signaling pathways (29), and because other Ad5 regulatory proteins alter posttranslational modifications, including protein ubiquitination and sumoylation (30, 31). His_6-SUMO3(T90R)-expressing HeLa cells (2×10^8) were infected with Ad5 or ΔE4-ORF3 for 7 h, harvested, and submitted to Cell Signaling Technology for PTMScan analysis using the K-ε-GG ubiquitin remnant motif antibody. We evaluated samples by Western blotting for SUMO2/3 and His_6-SUMO3(T90R) expression levels and global conjugation patterns. These patterns were the same with both virus infections (Fig. 2A). Ad5 E1A expression levels were also the same with both viruses, whereas the E4-ORF3 protein was only detected in cells infected with wild-type Ad5. The complete results of this analysis are presented in Table S1 in the supplemental material. A total of 7,792 redundant peptide assignments were made, with 4,477 nonredundant peptide assignments identified using the ubiquitin remnant motif antibody. The levels of the majority of these peptides (i.e., Ubl conjugation sites) were not changed in a statistically significant manner between the samples from cells infected with wild-type Ad5 versus those infected with ΔE4-ORF3. Cellular and Ad5 proteins whose K-ε-GG motif modification was changed ≥2-fold by E4-ORF3 expression and with a peptide intensity measurement

of >1,000,000 or that were changed ≥2.5-fold and with a peptide intensity measurement of >200,000 are listed in Table 1 according to the fold change from greatest to least, either increased (top group) or decreased (bottom group). A total of 166 K-ε-GG modification sites were identified in 51 proteins that were altered positively or negatively by Ad5 E4-ORF3 expression using these criteria. Modification at the majority of these sites (153/166) and in the majority of proteins (41/51) was increased in Ad5-infected cell samples compared to ΔE4-ORF3-infected cell samples. Most of these sites were identified in cellular proteins, but one was identified in the Ad5 DNA binding protein (DBP) (see Table S1 in the supplemental material). The number of conjugation sites identified in the 51 cellular proteins altered by E4-ORF3 expression ranged from only 1 site altered (28 proteins), 2 sites altered (10 proteins), 3 to 8 sites altered (9 proteins), to 10 or more sites altered (4 proteins). Among this list were Nbs1 and Mre11, which were previously identified as proteins whose SUMO2/3 conjugation is induced by Ad5 E4-ORF3 (11).

Ubiquitin and Nedd8 conjugation patterns and localization are not altered by Ad5 E4-ORF3. The analysis of a K-ε-GG linkage would identify SUMO3(T90R) conjugation sites but also may identify conjugation of ubiquitin itself, as well the Ubl proteins Nedd8 and ISG15, which all contain an arginine residue upstream of the diglycine conjugation site (Fig. 1A). The proteins identified in this study with K-ε-GG modifications regulated by E4-ORF3 are listed in Table S2 in the supplemental material, with known SUMO, ubiquitin, Nedd8, and ISG15 modifications listed and referenced. We analyzed whether E4-ORF3 expression altered global patterns of ubiquitin, Nedd8, and ISG15 protein conjugation by 7 h after infection. HeLa cells were infected with Ad5 or ΔE4-ORF3, and total cell lysates were prepared using denaturing conditions. Western blot analyses were performed using antibodies directed against ubiquitin, Nedd8, and ISG15 (Fig. 2B). The patterns of total ubiquitin or Nedd8 conjugation were indistinguishable following infection with either virus. ISG15 conjugation was not apparent in unstimulated HeLa cells but was induced following IFN-α treatment, consistent with the fact that ISG15 is an interferon-stimulated gene (ISG) product (32). Since Ad5 infection is known to alter the ubiquitination of a number of cellular substrates (4-6, 33-38), total ubiquitin conjugation patterns observed using whole-cell lysates were confirmed by immunoprecipitation (Fig. 2C). No changes were evident in cells infected with Ad5 or ΔE4-ORF3 in comparison to uninfected cells. The lack of change in global ubiquitin and Nedd8 conjugation patterns following E4-ORF3 expression was not surprising, since the same was true with global SUMO2/3 conjugation patterns (Fig. 2A). We had previously correlated the induction of SUMO conjugation to Mre11 and Nbs1 induced by the E4-ORF3 protein with the relocalization of SUMO1 and SUMO2/3 into E4-ORF3-containing nuclear tracks (11). Therefore, we examined the subcellular localization of ubiquitin and Nedd8 following infection of HeLa cells with Ad5 or ΔE4-ORF3. Wild-type Ad5 infection did not alter the subcellular distribution of ubiquitin or Nedd8 compared to uninfected cells at 7 h postinfection (Fig. 2D and E). We concluded that the Ad5 E4-ORF3 protein does not alter global patterns of ubiquitin, Nedd8, or ISG15 protein conjugation, or the subcellular localization of ubiquitin or Nedd8.

The Ad5 E4-ORF3 protein induces sumoylation of multiple cellular substrates. We next examined the conjugation of SUMO3 to several K-ε-GG conjugation substrates (listed in Table 1). Parental HeLa cells or His_6-SUMO3-expressing HeLa cells were left uninfected or infected with Ad5 or ΔE4-ORF3 for 7 h, and patterns of total SUMO3 conjugation or SUMO3 conjugation to specific substrates were examined (Fig. 3A and B). Patterns of total SUMO3 conjugation were not changed following infection with either virus in comparison to uninfected cells in whole-cell extracts (Fig. 3A, lysate) or in Ni-NTA-purified samples (Fig. 3A, His pulldown). RanGAP1 served as an internal control. Wild-type Ad5, but not ΔE4-ORF3, induced the conjugation of SUMO3 to Nbs1 and Mre11 with multiple sumoylated species evident (Fig. 3B, His pulldown), as we previously reported (11). Comparable levels of these proteins were evident in whole-cell extracts from uninfected and Ad-infected cells (lysate). Conjugation of SUMO3 to TIF1γ and PML was evident with uninfected cells and also was observed in cells infected with both viruses, with multiple sumoylated species observed in both cases (Fig. 3B). SUMO3 conjugation to TIF1γ, however, was augmented following infection with wild-type Ad5, in comparison to uninfected and ΔE4-ORF3-infected cells. No obvious differences were evident in the patterns of PML-SUMO3 conjugation following infection with wild-type Ad5 versus the E4-ORF3 mutant virus. Since multiple SUMO3-conjugated PML species were evident, it is difficult to determine if sumoylation was induced or if conjugation sites were altered during Ad infection using this assay.

A substrate whose modification is abundantly altered by E4-ORF3 expression is transcription factor II-I (TFII-I/GTF2-I), with 37 sites changed 2-fold or more. TFII-I has not been previously associated with E4-ORF3 function or Ad5 infection. As observed with TIF1γ and PML, TFII-I was sumoylated in uninfected cells, consistent with previous reports (14, 39) (Fig. 3B). Infection with wild-type Ad5, but not ΔE4-ORF3, augmented TFII-I sumoylation compared to uninfected cells (Fig. 3B). It is also possible that E4-ORF3-induced polysumoylation of TFII-I could account for the new higher-molecular-weight species observed in Ad5-infected cell extracts. Changes in TFII-I levels in Ad-infected cell extracts were not reproducibly observed. We also examined TFII-I subcellular localization in uninfected cells and wild-type Ad5- and ΔE4-ORF3-infected cells (Fig. 3C). A diffuse nuclear distribution was observed in uninfected cells and cells infected with the E4-ORF3 mutant virus. In contrast, TFII-I was relocalized into E4-ORF3 tracks following infection with wild-type Ad5. These results verify that wild-type Ad5 infection induces selective SUMO3 modification of cellular proteins and that TFII-I is a new cellular target of Ad5 E4-ORF3.

Finally, we compared the total K-ε-GG conjugation sites identified in this analysis to those regulated by E4-ORF3 and aligned these sites to determine if a consensus sequence exists for E4-ORF3 targeting (Fig. 4). Of the total K-ε-GG conjugation sites identified, 4,311 were not affected by E4-ORF3 expression, whereas 166 sites were affected (153 sites increased, 13 sites decreased). Of the total proteins with K-ε-GG conjugation sites identified, 1,669 were not affected by E4-ORF3 expression, whereas 51 proteins were affected (41 increased, 10 decreased) (Fig. 4A). Of the K-ε-GG conjugation sites affected by E4-ORF3 expression, there was no notable consensus motif identified with the total sites, or with sites whose modification was increased or decreased (Fig. 4B). SUMO conjugation by E3 ligases frequently involves nonconsensus lysine residues (12, 13).

TABLE 1 List of identified proteins

Protein		Uniprotkb accession no.	Gene name	No. of changed sites[a]	Highest fold change	Description
Abbreviation	Name					
GTF2I	General transcription factor II-I	P78347	GTF2I	37	126.9	Transcription, transcription regulation
RAD50	DNA repair protein RAD50	Q92878	RAD50	13	11.6	Cell cycle, DNA damage, DNA repair, meiosis
RPL27	60S ribosomal protein L27	P61353	RPL27	12	29.1	Ribonucleoprotein, ribosomal protein
SKAR	Polymerase delta-interacting protein 3	Q9BY77	POLDIP3	10	97.2	mRNA transport, translation regulation, transport
PML	Promyelocytic leukemia protein	P29590	PML	8	5.0	Immune response, apoptosis, transcription regulation
MRE11	Meiotic recombination 11	P49959	MRE11	7	46.5	DNA damage, DNA repair, meiosis
TIF1γ	Transcription intermediary factor 1-γ	Q9UPN9	TRIM33	6	28.6	Transcription, transcription regulation, Ubl conjugation pathway
UTP14	U3 small nucleolar RNA-associated protein 14	Q9BVJ6	UTP14	5	44.4	Ribosome biogenesis
C1orf124	SprT-like domain-containing protein Spartan	Q9H040	SPRTN	5	9.6	DNA damage, DNA repair
MORC3	MORC family CW-type zinc finger protein 3	Q14149	MORC3	4	7.8	Cell cycle regulation
RPS16	40S ribosomal protein S16	P62249	RPS16	4	7.8	Ribonucleoprotein, ribosomal protein
PRPF3	U4/U6 small nuclear ribonucleoprotein Prp3	O43395	PRPF3	3	34.6	mRNA processing, mRNA splicing
NBS1	Nijmegen breakage syndrome protein 1	O60934	NBN	3	12.8	Cell cycle, DNA damage, DNA repair, meiosis
ADNP	Activity-dependent neuroprotective protein	Q9H2P0	ADNP	2	26.3	Transcription, transcription regulation
DNAJC1	DnaJ(Hsp40) homolog subfamily C member 1	Q96KC8	DNAJC1	2	15.0	Translation regulation, protein folding
MMP1	Interstitial collagenase	P03956	MMP1	2	15.0	Collagen degradation, host-virus interaction
VPS29	Vacuolar protein sorting-associated protein 29	Q9UBQ0	VPS29	2	7.2	Protein transport
THAP11	THAP domain-containing protein 11	Q96EK4	THAP11	2	6.5	Transcription, transcription regulation
WDSOF1	WD repeat and SOF domain-containing protein 1	Q9NV06	DCAF13	2	6.1	Ribosome biogenesis, rRNA processing, Ubl conjugation pathway
PDE3A	cGMP-inhibited 3',5'-cyclic phosphodiesterase A	Q14432	PDE3A	2	3.8	Nucleotide metabolism
RPL18a	60S ribosomal protein L18a	Q02543	RPL18A	2	2.6	Ribonucleoprotein, ribosomal protein
ZC3H3	Zinc finger CCCH domain-containing protein 3	Q8IXZ2	ZC3H3	1	47.5	Regulation of mRNA export
RNF169	RING finger protein 169	Q8NCN4	RNF169	1	10.4	DNA damage, Ubl conjugation pathway
DBC-1	Cell cycle and apoptosis regulator protein 2	Q8N163	CCAR2	1	7.1	Apoptosis, cell cycle, DNA damage, mRNA processing
HCFC1	Host cell factor 1	P51610	HCFC1	1	4.9	Cell cycle, host-virus interaction
Titin	Titin, connectin	Q8WZ42	TTN	1	4.2	Protein kinase
Skip	Ski-interacting protein	Q13573	SNW1	1	4.1	Host-virus interaction, mRNA processing, transcription regulation
ZNF198	Zinc finger protein 198	Q9UBW7	ZMYM2	1	3.8	Transcription, transcription regulation
SUMO2	Small ubiquitin-related modifier 2	P61956	SUMO2	1	3.8	Ubl conjugation pathway
C1orf77	Chromatin target of PRMT1 protein	Q9Y3Y2	CHTOP	1	3.4	mRNA transport, transcription, transcription regulation
RNF168	RING finger protein 168	Q8IYW5	RNF168	1	3.1	DNA damage, DNA repair, Ubl conjugation pathway
eIF4a2	Eukaryotic initiation factor 4A-II	Q14240	EIF4A2	1	2.9	Host-virus interaction, protein biosynthesis
GATAD2A	GATA zinc finger domain-containing protein 2A	Q86YP4	GATAD2A	1	2.7	Transcription, transcription regulation
RPS25	40S ribosomal protein S25	P62851	RPS25	1	2.6	Ribonucleoprotein, ribosomal protein
RPL28	60S ribosomal protein L28	P46779	RPL28	1	2.6	Ribonucleoprotein, ribosomal protein
SUMO1	Small ubiquitin-related modifier 1	P63165	SUMO1	1	2.4	Ubl conjugation pathway
Cx43	Connexin-43	P17302	GJA1	1	2.3	Gap junction protein

(Continued on following page)

TABLE 1 (Continued)

Protein		Uniprotkb accession no.	Gene name	No. of changed sites[a]	Highest fold change	Description
Abbreviation	Name					
RPL4	60S ribosomal protein L4	P36578	RPL4	1	2.2	Ribonucleoprotein, ribosomal protein
TXNL1	Thioredoxin-like protein 1	O43396	TXNL1	1	2.1	Electron transport
RPL8	60S ribosomal protein L8	P62917	RPL8	1	2.1	Ribonucleoprotein, ribosomal protein
HIP	Hsc70-interacting protein	P50502	ST13	1	2.0	Protein folding
UBE2L3	Ubiquitin-conjugating enzyme E2 L3	P68036	UBE2L3	3	−3.3	Transcription, transcription regulation, Ubl conjugation pathway
UCP2	Mitochondrial uncoupling protein 2	P55851	UCP2	2	−2.1	Transport
UBE2Z	Ubiquitin-conjugating enzyme E2 Z	Q9H832	UBE2Z	1	−2.9	Apoptosis, Ubl conjugation pathway
PRDX6	Peroxiredoxin-6	P30041	PRDX6	1	−2.4	Lipid metabolism
SPEC1	CDC42 small effector protein 1	Q9NRR8	CDC42SE1	1	−2.3	Cell shape, phagocytosis
PPIA	Peptidyl-prolyl *cis-trans* isomerase A	P62937	PPIA	1	−2.1	Host-virus interaction
RNF122	RING finger protein 122	Q9H9V4	RNF122	1	−2.1	Membrane protein, Ubl conjugation pathway
CTNNB1	Catenin beta-1	P35222	CTNNB1	1	−2.0	Cell adhesion, transcription regulation, Wnt signaling pathway
SLC7A5	Solute carrier family 7 member 5	Q01650	SLC7A5	1	−2.0	Amino acid transport, differentiation, neurogenesis, transport
UBE1	Ubiquitin-like modifier-activating enzyme 1	P22314	UBA1	1	−2.0	Ubl conjugation pathway

[a] The number of identified K-ε-GG sites changed by E4-ORF3 expression. The table lists the cellular proteins whose K-ε-GG conjugation is regulated by the Ad5 E4-ORF3 protein. The 51 proteins are listed according to the fold change, from greatest to lowest, including increased (top group) and decreased (bottom group [negative values]) changes.

DISCUSSION

We previously described that the Ad5 E4-ORF3 protein induces sumoylation of Mre11 and Nbs1 (11). We observed multiple E4-ORF3-induced SUMO conjugates of Nbs1 and Mre11 (also observed in this study [Fig. 3B]). The mobilities in SDS-PAGE of the fastest-migrating sumoylated Nbs1 and Mre11 species were consistent with the conjugation of two SUMO moieties, based on the observation that each SUMO modification reduces protein mobility in an SDS-PAGE gel by ~20 kDa. We anticipated that the Nbs1 species represented independent sumoylation sites rather than polysumoylation at a single lysine residue, since the number of bands was the same with SUMO1 and SUMO2/3 and because SUMO1 is not reported to form multichain linkages (12, 13). Only SUMO2/3 linkages were found with Mre11 that could correspond to mono- or polysumoylation. The results of the present study identified multiple sites of Ubl conjugation to Mre11 and Nbs1 induced by Ad5 E4-ORF3: seven sites on Mre11 and three sites on Nbs1. Our results also revealed Ubl conjugation to the Mre11/Nbs1 binding partner Rad50, with 13 identified conjugation sites induced by E4-ORF3 expression (see Table S1 in the supplemental material). While our studies were ongoing, Hay and colleagues reported the use of a 293 cell line that stably expresses His_6-SUMO2-T90K and the use of the PTMScan ubiquitin remnant motif antibody to identify cellular proteins conjugated to SUMO2 following heat shock (39). That analysis identified 1,002 sumoylated peptides in 539 substrate proteins. Interestingly, there was little overlap between the SUMO2 conjugation sites identified in their study in comparison to K-ε-GG conjugation sites identified in the present study, with overlap found with only 11 conjugation sites in five different proteins (TFII-I, Mre11, TIF1, UTP14, and SUMO2 [see Table S3 in the supplemental material]). Two SUMO conjugation sites were identified in Mre11 following heat shock that corresponded to two of the seven sites identified in the present study (K255 and K416). No SUMO conjugation sites were identified in Nbs1 or Rad50 following heat shock, compared to 16 total sites in these two proteins induced by Ad5 E4-ORF3 expression. Sumoylation of all three MRN components, Mre11, Rad50, and Xrs2 (Nbs1), was observed in *Saccharomyces cerevisiae* following the induction of a DDR by replicative stress. Protein sumoylation induced by a DDR is widespread in this organism (40). The yeast MRX complex serves as a positive regulator of sumoylation, and sumoylation significantly promotes the DDR in this system (40). Ribet and colleagues also recently reported the use of HeLa cell lines that stably express His_6-SUMO1-T95R and His_6-SUMO2-T91R and use of the PTMScan ubiquitin remnant motif antibody to identify cellular proteins constitutively conjugated to SUMO1 or SUMO2 (41). That analysis identified 295 SUMO1-conjugated peptides in 227 substrate proteins and 167 SUMO2-conjugated sites in 135 substrate proteins. Only two of these conjugation sites overlapped with those identified in the current study, one in TFII-I and one in TIF1γ (see Table S3).

Ubiquitination and sumoylation have emerged as important posttranslational modifications that regulate DDRs and DNA repair (42). Proliferating cell nuclear antigen (PCNA) is sumoylated at residue K164 during S phase, which recruits the DNA helicase Srs2 via a SUMO interaction motif (SIM) to restrict DNA recombination (43). The SUMOs (SUMO-1, SUMO-2, and SUMO-3), as well as components of the SUMO machinery, accumulate at sites of DNA damage to direct the sumoylation of proteins involved in DNA repair, such as BRCA (44, 45). Sumoylation increases BRCA1 Ub ligase activity. The E3 SUMO ligases protein inhibitor of activated STAT 1 and 4 (PIAS1 and PIAS4) localize at sites of DNA damage and are required for efficient DNA repair and recruitment of other effectors involved in a DDR (44, 45). Ad5 E4-ORF3 expression altered K-ε-GG conjugation of 51 cellular proteins identified in this study, mostly by inducing (41/51 substrates) rather than reducing this modification. The induction of K-ε-GG modification of the MRN components by E4-ORF3 was

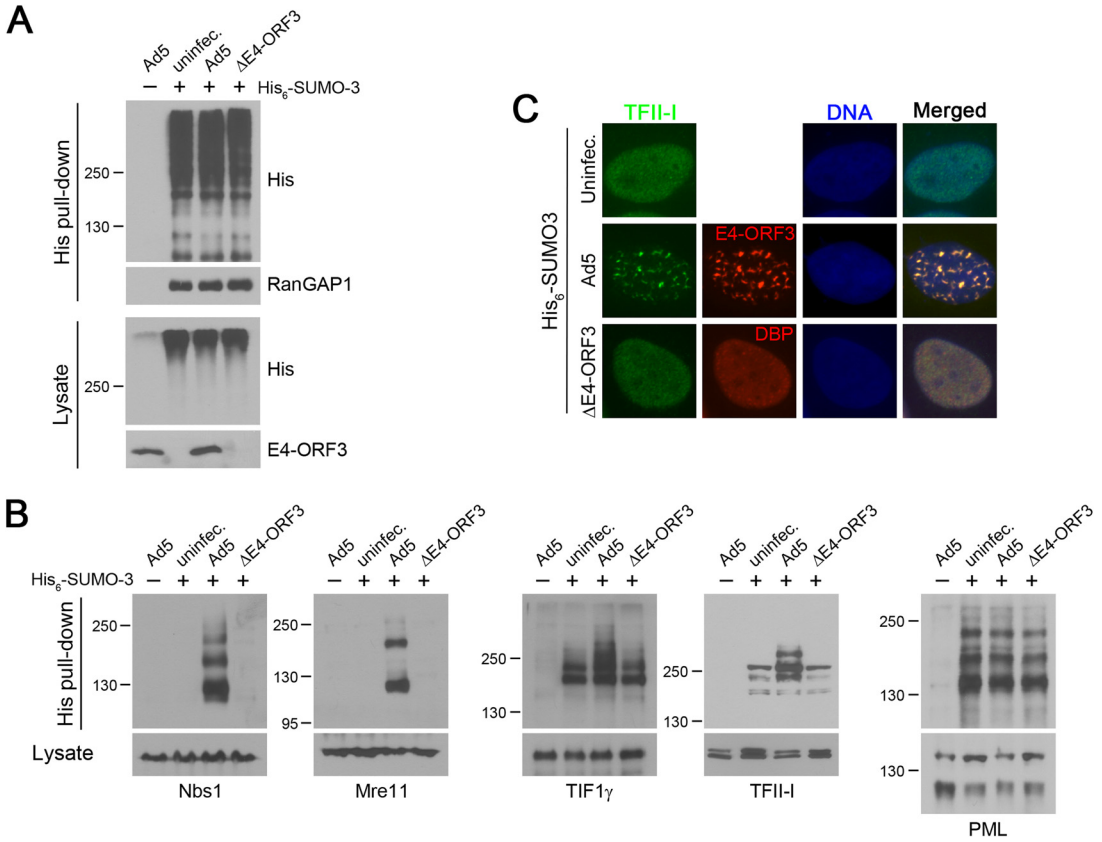

FIG 3 Verification of proteomic analysis. (A and B) Parental HeLa cells (–) and His_6-SUMO3-expressing HeLa cells (+) were left uninfected or infected with wild-type or E4-ORF3-deficient Ad5 for 7 h. SUMO3 conjugates were prepared using Ni-NTA–agarose beads under denaturing conditions followed by Western blotting with anti-His (A) and anti-Nbs1, -Mre11, -TIF1, -TFII-I, and -PML (B) antibodies. RanGAP1 was used as a sumoylation control for the blot in panel A. (C) Subcellular localization of TFII-I in uninfected cells or cells infected for 7 h with wild-type or E4-ORF3-deficient Ad5. TFII-I was immunostained using an anti-TFII-I antibody. E4-ORF3 and E2-DBP were used as markers of infected cells. Nuclei were visualized by DAPI staining (DNA).

particularly notable, since Mre11, Nbs1, and Rad50 represented 7.3% of the total proteins whose modification was increased by E4-ORF3, whereas K-ε-GG conjugation sites identified on these proteins represented 15% of the total modifications induced by E4-ORF3. Inhibition of the DDR during Ad infection is critical for successful virus replication (1, 2), and we propose that sumoylation of the MRN components promotes this process. The identification of specific SUMO3-conjugated lysine residues in these substrates will facilitate functional analyses in the future.

A second group of cellular proteins with K-ε-GG modification induced by Ad5 E4-ORF3 contained two proteins in the TRIM (TRIpartite Motif) family, PML (TRIM19) and TIF1γ (TRIM33). Both proteins are known binding partners of Ad5 E4-ORF3 (46, 47), but the induction of their sumoylation by E4-ORF3 was not previously reported. E4-ORF3 induced SUMO3 conjugation at eight sites in PML and six sites in TIF1γ. Again, these two SUMO3 substrates are overrepresented in our data set, where they represent 4.8% of the proteins whose modification was regulated by E4-ORF3 but contain 9.2% of the total K-ε-GG conjugation sites. TRIM family proteins are involved in intrinsic and interferon-induced antiviral immunity (48). PML inhibits immediate-early gene expression and viral replication of human herpesviruses herpes simplex virus 1 and human cytomegalovirus (49). Both of these viruses have evolved mechanisms to prevent PML restriction of viral replication. The Ad E4-ORF3 protein relocalizes PML and associated components Daxx and Sp100 into nuclear tracks to sequester their activities (9, 10). In the absence of E4-ORF3, interferons block viral early gene expression and viral DNA replication (9, 10). The induction of PML sumoylation by E4-ORF3 may be involved in this process, since PML sumoylation and the interaction of PML with SUMO through SUMO interaction motifs (SIMs) regulates PML-NB formation (50). It is an attractive hypothesis that Ad5 E4-ORF3 regulates cellular protein sumoylation to disrupt PML-NBs, as well as to recruit PML, PML-associated proteins, and other cellular effectors into E4-ORF3 nuclear tracks. Of the cellular proteins previously reported to be associated with E4-ORF3 nuclear tracks, most were identified in this study, including Mre11, Rad50, Nbs1, PML, and TIF1γ. However, several other cellular proteins known to associate with E4-ORF3 were not identified in these studies (e.g., Daxx, Sp100, TIF1α). If the induction of SUMO modification is involved in E4-ORF3 recruitment of cellular proteins into nuclear tracks, it is possible that Daxx, Sp100, and TIF1α are relocalized during Ad infection via alternative protein-protein interactions, such as the interaction of PML with Daxx and Sp100 (51) or the interaction of TIF1α with TIF1γ (52).

TFII-I was abundantly modified following Ad5 E4-ORF3 expression, with a total of 37 K-ε-GG conjugation sites identified (see Table S1 in the supplemental material). We verified that E4-ORF3 induces TFII-I sumoylation, with one or more additional

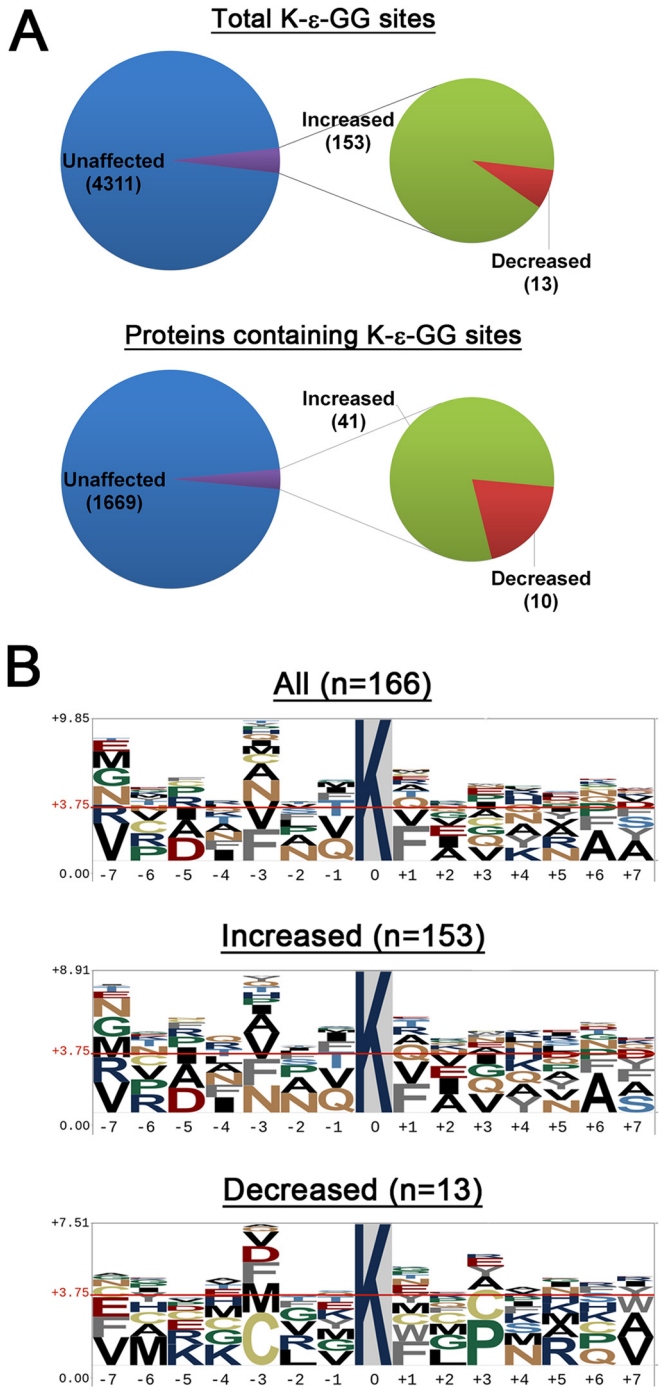

FIG 4 Profiling of K-ε-GG sites whose sumoylation was affected by Ad5 E4-ORF3 expression. (A) Pie charts show the numbers (and proportions) of unaffected and affected K-ε-GG site numbers (top) and proteins (bottom). (B) Results of E4-ORF3-affected K-ε-GG motif analysis (pLogo) (62). Seven residues neighboring all affected K-ε-GG sites (top) and increased (middle) and decreased (bottom) sites are shown. The *y* axis represents the log odds of the binominal probability. The red line indicates the threshold.

SUMO3 conjugates detected (Fig. 3B). TFII-I was also found to relocalize to E4-ORF3 nuclear tracks following wild-type Ad5 infection (Fig. 3C). In addition to TFII-I sumoylation, Ub conjugation to TFII-I has been reported for 11 of the 37 K-ε-GG sites identified in the present analysis (53, 54) (see Table S3 in the supplemental material). Therefore, some of the sites identified here may represent ubiquitin conjugation rather than SUMO conjugation. Twelve SUMO2 conjugation sites on TFII-I also were observed following heat shock (39), with six of these sites overlapping with those identified in the current analysis (see Table S3). TFII-I plays a role in numerous signaling pathways that regulate cellular gene expression, including transforming growth factor β, calcium, and stress signaling (55). TFII-I interacts with PIASx (Miz1/Siz2), an E3 SUMO ligase, and histone deacetylase 3 (HDAC3), as part of a transcriptional activating complex (56, 57). How TFII-I activity may be regulated in response to signaling events and by sumoylation is not known.

The remainder of the proteins with K-ε-GG modifications induced by E4-ORF3 fell into a number of different functional categories and may, or may not, represent bona fide E4-ORF3 sumoylation targets. We favor the view that many of the modification sites identified in this analysis, in fact, represent E4-ORF3-induced sumoylation, since we previously found a strict correlation between relocalization of SUMO proteins into E4-ORF3-containing nuclear tracks and the ability of E4-ORF3 to direct sumoylation of Mre11 and Nbs1 (11). Since the subcellular localizations of ubiquitin and Nedd8 were not altered by E4-ORF3 expression (Fig. 2D and E), it appears that these proteins may not be positioned appropriately in infected cell nuclei to be conjugated to substrates recruited by the E4-ORF3 protein. Table S3 displays all of the E4-ORF-induced K-ε-GG conjugation sites identified in the present study with overlapping sites within these proteins known to be sites of ubiquitin conjugation identified in large-scale proteomic analyses (22, 53, 54). The latter two referenced studies utilized the K-ε-GG antibody from Cell Signaling Technology to identify proteins conjugated to ubiquitin and conjugation sites. Fifty-four of the 166 K-ε-GG conjugation sites identified in the present study were also identified as ubiquitin conjugation sites. While there is overlap with one-third of the K-ε-GG conjugation sites identified in the present study, two-thirds of the K-ε-GG conjugation sites induced by E4-ORF3 are unique and likely represent protein sumoylation. Finally, we note that the TIF1 family members TIF1β (TRIM28) and TIF1γ (TRIM33) have intrinsic SUMO E3 ligase activities, as do several other TRIM family members (58–61). One or more of these proteins may play a role in E4-ORF3-induced sumoylation *in vivo*. We also cannot rule out the possibility that the E4-ORF3 protein itself possesses SUMO ligase activity. Future analyses will be required to determine how the E4-ORF3 protein regulates the K-ε-GG modification of cellular substrates and the functional consequences of these events.

ACKNOWLEDGMENTS

We are very grateful to Ronald Hay (University of Dundee) for providing His_6-SUMO cell lines and other reagents. We thank Thomas Dobner (Heinrich-Pette Institute) for the anti-E4-ORF3 monoclonal antibody (6A-11), Arnold Levine (Princeton University) for the anti-DBP (B6-8) monoclonal antibody, and Peter van der Vliet (University of Utrecht) for the rabbit polyclonal anti-DBP antibody. We thank Dafna Bar-Sagi for the ubiquitin expression vector and Matthias Dobbelstein for the Nedd8 expression vector. We are grateful to Jeffrey Silva at Cell Signaling Technology for informational discussions of the proteomic approach and analysis, and we thank members of our laboratory for informed discussions.

This work was supported by NIH grant CA122677. R.G.B. was supported by NIH training grants T32CA009176 and T32AI007539.

REFERENCES

1. **Weitzman MD, Lilley CE, Chaurushiya MS.** 2010. Genomes in conflict: maintaining genome integrity during virus infection. Annu Rev Microbiol **64:**61–81. http://dx.doi.org/10.1146/annurev.micro.112408.134016.
2. **Weitzman MD, Ornelles DA.** 2005. Inactivating intracellular antiviral responses during adenovirus infection. Oncogene **24:**7686–7696. http://dx.doi.org/10.1038/sj.onc.1209063.
3. **Karen KA, Hearing P.** 2011. Adenovirus core protein VII protects the viral genome from a DNA damage response at early times after infection. J Virol **85:**4135–4142. http://dx.doi.org/10.1128/JVI.02540-10.
4. **Harada JN, Shevchenko A, Pallas DC, Berk AJ.** 2002. Analysis of the adenovirus E1B-55K-anchored proteome reveals its link to ubiquitination machinery. J Virol **76:**9194–9206. http://dx.doi.org/10.1128/JVI.76.18.9194-9206.2002.
5. **Querido E, Blanchette P, Yan Q, Kamura T, Morrison M, Boivin D, Kaelin WG, Conaway RC, Conaway JW, Branton PE.** 2001. Degradation of p53 by adenovirus E4orf6 and E1B55K proteins occurs via a novel mechanism involving a Cullin-containing complex. Genes Dev **15:**3104–3117. http://dx.doi.org/10.1101/gad.926401.
6. **Stracker TH, Carson CT, Weitzman MD.** 2002. Adenovirus oncoproteins inactivate the Mre11-Rad50-NBS1 DNA repair complex. Nature **418:**348–352. http://dx.doi.org/10.1038/nature00863.
7. **Doucas V, Ishov AM, Romo A, Juguilon H, Weitzman MD, Evans RM, Maul GG.** 1996. Adenovirus replication is coupled with the dynamic properties of the PML nuclear structure. Genes Dev **10:**196–207. http://dx.doi.org/10.1101/gad.10.2.196.
8. **Evans JD, Hearing P.** 2005. Relocalization of the Mre11-Rad50-Nbs1 complex by the adenovirus E4 ORF3 protein is required for viral replication. J Virol **79:**6207–6215. http://dx.doi.org/10.1128/JVI.79.10.6207-6215.2005.
9. **Ullman AJ, Hearing P.** 2008. Cellular proteins PML and Daxx mediate an innate antiviral defense antagonized by the adenovirus E4 ORF3 protein. J Virol **82:**7325–7335. http://dx.doi.org/10.1128/JVI.00723-08.
10. **Ullman AJ, Reich NC, Hearing P.** 2007. Adenovirus E4 ORF3 protein inhibits the interferon-mediated antiviral response. J Virol **81:**4744–4752. http://dx.doi.org/10.1128/JVI.02385-06.
11. **Sohn SY, Hearing P.** 2012. Adenovirus regulates sumoylation of Mre11-Rad50-Nbs1 components through a paralog-specific mechanism. J Virol **86:**9656–9665. http://dx.doi.org/10.1128/JVI.01273-12.
12. **Citro S, Chiocca S.** 2013. Sumo paralogs: redundancy and divergencies. Front Biosci **5:**544–553. https://www.bioscience.org/2013/v5s/af/388/fulltext.htm.
13. **Hay RT.** 2013. Decoding the SUMO signal. Biochem Soc Trans **41:**463–473. http://dx.doi.org/10.1042/BST20130015.
14. **Becker J, Barysch SV, Karaca S, Dittner C, Hsiao HH, Berriel Diaz M, Herzig S, Urlaub H, Melchior F.** 2013. Detecting endogenous SUMO targets in mammalian cells and tissues. Nat Struct Mol Biol **20:**525–531. http://dx.doi.org/10.1038/nsmb.2526.
15. **Blomster HA, Hietakangas V, Wu J, Kouvonen P, Hautaniemi S, Sistonen L.** 2009. Novel proteomics strategy brings insight into the prevalence of SUMO-2 target sites. Mol Cell Proteomics **8:**1382–1390. http://dx.doi.org/10.1074/mcp.M800551-MCP200.
16. **Blomster HA, Imanishi SY, Siimes J, Kastu J, Morrice NA, Eriksson JE, Sistonen L.** 2010. In vivo identification of sumoylation sites by a signature tag and cysteine-targeted affinity purification. J Biol Chem **285:**19324–19329. http://dx.doi.org/10.1074/jbc.M110.106955.
17. **Bruderer R, Tatham MH, Plechanovova A, Matic I, Garg AK, Hay RT.** 2011. Purification and identification of endogenous polySUMO conjugates. EMBO Rep **12:**142–148. http://dx.doi.org/10.1038/embor.2010.206.
18. **Da Silva-Ferrada E, Xolalpa W, Lang V, Aillet F, Martin-Ruiz I, de la Cruz-Herrera CF, Lopitz-Otsoa F, Carracedo A, Goldenberg SJ, Rivas C, England P, Rodriguez MS.** 2013. Analysis of SUMOylated proteins using SUMO-traps. Sci Rep **3:**1690. http://dx.doi.org/10.1038/srep01690.
19. **Galisson F, Mahrouche L, Courcelles M, Bonneil E, Meloche S, Chelbi-Alix MK, Thibault P.** 2011. A novel proteomics approach to identify SUMOylated proteins and their modification sites in human cells. Mol Cell Proteomics **10:**M110.004796. http://dx.doi.org/10.1074/mcp.M110.004796.
20. **Tatham MH, Rodriguez MS, Xirodimas DP, Hay RT.** 2009. Detection of protein SUMOylation in vivo. Nat Protoc **4:**1363–1371. http://dx.doi.org/10.1038/nprot.2009.128.
21. **Knuesel M, Cheung HT, Hamady M, Barthel KK, Liu X.** 2005. A method of mapping protein sumoylation sites by mass spectrometry using a modified small ubiquitin-like modifier 1 (SUMO-1) and a computational program. Mol Cell Proteomics **4:**1626–1636. http://dx.doi.org/10.1074/mcp.T500011-MCP200.
22. **Lee KA, Hammerle LP, Andrews PS, Stokes MP, Mustelin T, Silva JC, Black RA, Doedens JR.** 2011. Ubiquitin ligase substrate identification through quantitative proteomics at both the protein and peptide levels. J Biol Chem **286:**41530–41538. http://dx.doi.org/10.1074/jbc.M111.248856.
23. **Nevels M, Täuber B, Kremmer E, Spruss T, Wolf H, Dobner T.** 1999. Transforming potential of the adenovirus type 5 E4orf3 protein. J Virol **73:**1591–1600.
24. **Vink EI, Yondola MA, Wu K, Hearing P.** 2012. Adenovirus E4-ORF3-dependent relocalization of TIF1α and TIF1γ relies on access to the coiled-coil motif. Virology **422:**317–325. http://dx.doi.org/10.1016/j.virol.2011.10.033.
25. **Olsen JV, de Godoy LM, Li G, Macek B, Mortensen P, Pesch R, Makarov A, Lange O, Horning S, Mann M.** 2005. Parts per million mass accuracy on an Orbitrap mass spectrometer via lock mass injection into a C-trap. Mol Cell Proteomics **4:**2010–2021. http://dx.doi.org/10.1074/mcp.T500030-MCP200.
26. **Lundgren DH, Martinez H, Wright ME, Han DK.** 2009. Protein identification using Sorcerer 2 and SEQUEST. Curr Protoc Bioinformatics Chapter 13:Unit 13.3. http://dx.doi.org/10.1002/0471250953.bi1303s28.
27. **Guo A, Gu H, Zhou J, Mulhern D, Wang Y, Lee KA, Yang V, Aguiar M, Kornhauser J, Jia X, Ren J, Beausoleil SA, Silva JC, Vemulapalli V, Bedford MT, Comb MJ.** 2014. Immunoaffinity enrichment and mass spectrometry analysis of protein methylation. Mol Cell Proteomics **13:**372–387. http://dx.doi.org/10.1074/mcp.O113.027870.
28. **Stokes MP, Farnsworth CL, Moritz A, Silva JC, Jia X, Lee KA, Guo A, Polakiewicz RD, Comb MJ.** 2012. PTMScan direct: identification and quantification of peptides from critical signaling proteins by immunoaffinity enrichment coupled with LC-MS/MS. Mol Cell Proteomics 11:187–201. http://dx.doi.org/10.1074/mcp.M111.015883.
29. **Wolfrum N, Greber UF.** 2013. Adenovirus signalling in entry. Cell Microbiol **15:**53–62. http://dx.doi.org/10.1111/cmi.12053.
30. **Blanchette P, Branton PE.** 2009. Manipulation of the ubiquitin-proteasome pathway by small DNA tumor viruses. Virology **384:**317–323. http://dx.doi.org/10.1016/j.virol.2008.10.005.
31. **Wimmer P, Blanchette P, Schreiner S, Ching W, Groitl P, Berscheminski J, Branton PE, Will H, Dobner T.** 2013. Cross-talk between phosphorylation and SUMOylation regulates transforming activities of an adenoviral oncoprotein. Oncogene **32:**1626–1637. http://dx.doi.org/10.1038/onc.2012.187.
32. **Zhao C, Collins MN, Hsiang TY, Krug RM.** 2013. Interferon-induced ISG15 pathway: an ongoing virus-host battle. Trends Microbiol **21:**181–186. http://dx.doi.org/10.1016/j.tim.2013.01.005.
33. **Baker A, Rohleder KJ, Hanakahi LA, Ketner G.** 2007. Adenovirus E4 34k and E1b 55k oncoproteins target host DNA ligase IV for proteasomal degradation. J Virol **81:**7034–7040. http://dx.doi.org/10.1128/JVI.00029-07.
34. **Blackford AN, Patel RN, Forrester NA, Theil K, Groitl P, Stewart GS, Taylor AM, Morgan IM, Dobner T, Grand RJ, Turnell AS.** 2010. Adenovirus 12 E4orf6 inhibits ATR activation by promoting TOPBP1 degradation. Proc Natl Acad Sci U S A **107:**12251–12256. http://dx.doi.org/10.1073/pnas.0914605107.
35. **Dallaire F, Blanchette P, Groitl P, Dobner T, Branton PE.** 2009. Identification of integrin α3 as a new substrate of the adenovirus E4orf6/E1B 55-kilodalton E3 ubiquitin ligase complex. J Virol **83:**5329–5338. http://dx.doi.org/10.1128/JVI.00089-09.
36. **Gupta A, Jha S, Engel DA, Ornelles DA, Dutta A.** 2013. Tip60 degradation by adenovirus relieves transcriptional repression of viral transcriptional activator EIA. Oncogene **32:**5017–5025. http://dx.doi.org/10.1038/onc.2012.534.
37. **Orazio NI, Naeger CM, Karlseder J, Weitzman MD.** 2011. The adenovirus E1b55K/E4orf6 complex induces degradation of the Bloom helicase during infection. J Virol **85:**1887–1892. http://dx.doi.org/10.1128/JVI.02134-10.
38. **Schreiner S, Wimmer P, Sirma H, Everett RD, Blanchette P, Groitl P, Dobner T.** 2010. Proteasome-dependent degradation of Daxx by the viral E1B-55K protein in human adenovirus-infected cells. J Virol **84:**7029–7038. http://dx.doi.org/10.1128/JVI.00074-10.

39. **Tammsalu T, Matic I, Jaffray EG, Ibrahim AF, Tatham MH, Hay RT.** 2014. Proteome-wide identification of SUMO2 modification sites. Sci Signal **7:**rs2. http://dx.doi.org/10.1126/scisignal.2005146.
40. **Cremona CA, Sarangi P, Yang Y, Hang LE, Rahman S, Zhao X.** 2012. Extensive DNA damage-induced sumoylation contributes to replication and repair and acts in addition to the mec1 checkpoint. Mol Cell **45:**422–432. http://dx.doi.org/10.1016/j.molcel.2011.11.028.
41. **Impens F, Radoshevich L, Cossart P, Ribet D.** 2014. Mapping of SUMO sites and analysis of SUMOylation changes induced by external stimuli. Proc Natl Acad Sci U S A **111:**12432–12437. http://dx.doi.org/10.1073/pnas.1413825111.
42. **Jackson SP, Durocher D.** 2013. Regulation of DNA damage responses by ubiquitin and SUMO. Mol Cell **49:**795–807. http://dx.doi.org/10.1016/j.molcel.2013.01.017.
43. **Fox JT, Lee KY, Myung K.** 2011. Dynamic regulation of PCNA ubiquitylation/deubiquitylation. FEBS Lett **585:**2780–2785. http://dx.doi.org/10.1016/j.febslet.2011.05.053.
44. **Galanty Y, Belotserkovskaya R, Coates J, Polo S, Miller KM, Jackson SP.** 2009. Mammalian SUMO E3-ligases PIAS1 and PIAS4 promote responses to DNA double-strand breaks. Nature **462:**935–939. http://dx.doi.org/10.1038/nature08657.
45. **Morris JR, Boutell C, Keppler M, Densham R, Weekes D, Alamshah A, Butler L, Galanty Y, Pangon L, Kiuchi T, Ng T, Solomon E.** 2009. The SUMO modification pathway is involved in the BRCA1 response to genotoxic stress. Nature **462:**886–890. http://dx.doi.org/10.1038/nature08593.
46. **Hoppe A, Beech SJ, Dimmock J, Leppard KN.** 2006. Interaction of the adenovirus type 5 E4 Orf3 protein with promyelocytic leukemia protein isoform II is required for ND10 disruption. J Virol **80:**3042–3049. http://dx.doi.org/10.1128/JVI.80.6.3042-3049.2006.
47. **Yondola MA, Hearing P.** 2007. The adenovirus E4 ORF3 protein binds and reorganizes the TRIM family member transcriptional intermediary factor 1 alpha. J Virol **81:**4264–4271. http://dx.doi.org/10.1128/JVI.02629-06.
48. **Rajsbaum R, Garcia-Sastre A, Versteeg GA.** 2014. TRIMmunity: the roles of the TRIM E3-ubiquitin ligase family in innate antiviral immunity. J Mol Biol **426:**1265–1284. http://dx.doi.org/10.1016/j.jmb.2013.12.005.
49. **Glass M, Everett RD.** 2013. Components of promyelocytic leukemia nuclear bodies (ND10) act cooperatively to repress herpesvirus infection. J Virol **87:**2174–2185. http://dx.doi.org/10.1128/JVI.02950-12.
50. **Shen TH, Lin HK, Scaglioni PP, Yung TM, Pandolfi PP.** 2006. The mechanisms of PML-nuclear body formation. Mol Cell **24:**331–339. http://dx.doi.org/10.1016/j.molcel.2006.09.013.
51. **Maul GG, Negorev D, Bell P, Ishov AM.** 2000. Review: properties and assembly mechanisms of ND10, PML bodies, or PODs. J Struct Biol **129:**278–287. http://dx.doi.org/10.1006/jsbi.2000.4239.
52. **Peng H, Feldman I, Rauscher FJ, III.** 2002. Hetero-oligomerization among the TIF family of RBCC/TRIM domain-containing nuclear cofactors: a potential mechanism for regulating the switch between coactivation and corepression. J Mol Biol **320:**629–644. http://dx.doi.org/10.1016/S0022-2836(02)00477-1.
53. **Kim W, Bennett EJ, Huttlin EL, Guo A, Li J, Possemato A, Sowa ME, Rad R, Rush J, Comb MJ, Harper JW, Gygi SP.** 2011. Systematic and quantitative assessment of the ubiquitin-modified proteome. Mol Cell **44:**325–340. http://dx.doi.org/10.1016/j.molcel.2011.08.025.
54. **Wagner SA, Beli P, Weinert BT, Nielsen ML, Cox J, Mann M, Choudhary C.** 2011. A proteome-wide, quantitative survey of in vivo ubiquitylation sites reveals widespread regulatory roles. Mol Cell Proteomics **10:**M111.013284. http://dx.doi.org/10.1074/mcp.M111.013284.
55. **Roy AL.** 2012. Biochemistry and biology of the inducible multifunctional transcription factor TFII-I: 10 years later. Gene **492:**32–41. http://dx.doi.org/10.1016/j.gene.2011.10.030.
56. **Tussie-Luna M, Bayarsaihan D, Seto E, Ruddle FH, Roy AL.** 2002. Physical and functional interactions of histone deacetylase 3 with TFII-I family proteins and PIASxbeta. Proc Natl Acad Sci U S A **99:**12807–12812. http://dx.doi.org/10.1073/pnas.192464499.
57. **Tussie-Luna MI, Michel B, Hakre S, Roy AL.** 2002. The SUMO ubiquitin-protein isopeptide ligase family member Miz1/PIASxbeta/Siz2 is a transcriptional cofactor for TFII-I. J Biol Chem **277:**43185–43193. http://dx.doi.org/10.1074/jbc.M207635200.
58. **Chu Y, Yang X.** 2011. SUMO E3 ligase activity of TRIM proteins. Oncogene **30:**1108–1116. http://dx.doi.org/10.1038/onc.2010.462.
59. **Ikeuchi Y, Dadakhujaev S, Chandhoke AS, Huynh MA, Oldenborg A, Ikeuchi M, Deng L, Bennett EJ, Harper J W, Bonni A, Bonni S.** 2014. TIF1gamma protein regulates epithelial-mesenchymal transition by operating as a small ubiquitin-like modifier (SUMO) E3 ligase for the transcriptional regulator SnoN1. J Biol Chem **289:**25067–25078. http://dx.doi.org/10.1074/jbc.M114.575878.
60. **Ivanov AV, Peng H, Yurchenko V, Yap KL, Negorev DG, Schultz DC, Psulkowski E, Fredericks WJ, White DE, Maul GG, Sadofsky MJ, Zhou MM, Rauscher FJ, III.** 2007. PHD domain-mediated E3 ligase activity directs intramolecular sumoylation of an adjacent bromodomain required for gene silencing. Mol Cell **28:**823–837. http://dx.doi.org/10.1016/j.molcel.2007.11.012.
61. **Liang Q, Deng H, Li X, Wu X, Tang Q, Chang TH, Peng H, Rauscher FJ, III, Ozato K, Zhu F.** 2011. Tripartite motif-containing protein 28 is a small ubiquitin-related modifier E3 ligase and negative regulator of IFN regulatory factor 7. J Immunol **187:**4754–4763. http://dx.doi.org/10.4049/jimmunol.1101704.
62. **O'Shea JP, Chou MF, Quader SA, Ryan JK, Church GM, Schwartz D.** 2013. pLogo: a probabilistic approach to visualizing sequence motifs. Nat Methods **10:**1211–1212. http://dx.doi.org/10.1038/nmeth.2646.